A NOVEL PORT-HAMILTONIAN BASED DESIGN OF STABILIZING CONTROLLER FOR DC-DC BUCK CONVERTERS

Juan Tomassini[(a)], Alejandro Donaire[(b)], Sergio Junco[(c)]

[(a),(c)] LAC, Laboratorio de Automatización y Control, Departamento de Control, Escuela de Ingeniería Electrónica, Facultad de Ciencias Exactas e Ingeniería, Universidad Nacional de Rosario, Argentina.
[(b)] Institute for Future Environments, School of Electrical Engineering and Computer Science Science, Queensland University of Technology, Australia.

[(a)]tomajuan@fceia.unr.edu.ar, [(b)]alejandro.donaire@qut.edu.au, [(c)]sjunco@fceia.unr.edu.ar

ABSTRACT
In this work we present a port-Hamiltonian supported control system design aimed at stabilizing a DC-DC Buck converter driving a nonlinear dissipative load. A desired closed-loop dynamics in the form of a port-Hamiltonian system is proposed, whose parameterization enforces the asymptotic stability of the desired equilibrium point. Moreover, the closed loop incorporates a first order dynamic extension allowing to reject constant disturbances on the load side. We prove that the closed loop is ISS respect to unmatched disturbances. To extend this property to disturbances acting on the supply side we add a standard PI output regulator to the previous closed loop. The performance of the closed loop is verified via simulation.

Keywords: DC-DC Buck converter, averaged models, passivity-based control, port-Hamiltonian systems.

1. INTRODUCTION

Due to their versatility, high efficiency, controllable behaviour, fast dynamics and wide-range of power management, Power Electronic Converters (PEC) are ubiquitous and pervade most of the cutting-edge engineering application areas. Indeed, they can be found in electrical drives, switched-mode power supplies, battery chargers, uninterrupted power supplies, all type of mobile devices, distributed generation and renewable energy conversion systems, embedded in electric/hybrid vehicles (cars, trains and airplanes), etc. (F. Dong Tan 2013).

Closed-loop control of PEC is mandatory when their mission is the conditioning of the processed or the output power subject to hard application specifications and under the effect of significant disturbances. Model-based control system synthesis methods are required for high-performance behaviour. From a Modelling point of view, PEC are hybrid, non linear systems composed of continuous elements like inductors, capacitors, resistors, sources, etc., and switching devices allowing for the control actions, like transistors, diodes, etc. As opposed to hybrids associating continuous-variables (with continuous- or discrete-time) and discrete-event models, the vast majority of techniques employed to perform dynamic analysis and control system synthesis are developed on averaged continuous models of PEC. A further division concerns the direct use of nonlinear averaged models or their linearizations around a desired equilibrium point. Linear controllers are tuned for specific operating points and, unless complemented with adaptation mechanisms –what adds complexity to the controller–, the closed-loop performance degrades when the operating point changes. Nonlinear controllers with a unique parameterization valid for the whole operating range are thus preferable, see for instance (Bacha, Munteanu and Bratcu 2014). Exact feedback-linearization, passivity-based control and Lyapunov-like stabilization count among the continuous-time control techniques derived on nonlinear averaged continuous converter models (Sira-Ramírez and Silva-Ortigoza 2006).

Through its application to the control of a Buck converter, this paper presents a method to address these kinds of problems in the modelling framework known as pH systems (PHS), see (Ortega, van der Schaft, Maschke and Escobar, 2002). The rationale of our technique is to find a control law that renders the closed-loop dynamics as a desired PHS, which incorporates a first order extension of the original dynamics. The associated storage function qualifies as a Lyapunov function, therefore guaranteeing the stability of the closed-loop. The resultant feedback law is a controller robust in face of parameter uncertainty and load-side varying bounded disturbances. As it is not robust respect to supply-side disturbances, a second robustifying PI-output regulator is added, which rejects piece-wise constant disturbances.

The remainder of the paper is organized as follows: Section 2 presents the averaged model of the Buck converter and the control system objectives. Section 3 deals with the design of the control system and the derivation of the control law. The behaviour of the overall control law is demonstrated in Section 4 with the help of simulation results in different scenarios, including state-dependent and external disturbances. Finally, Section 5 presents the conclusions.

2. PROBLEM FORMULATION

This section first introduces the topology of the switched converter as well as its averaged nonlinear model and then specifies the control problem to be solved.

2.1. System Model

The idealized equivalent switched circuit of the DC-DC Buck converter is first introduced followed by the average state-equation model employed for the controller design. Only the continuous-conduction mode (CCM) of the inductor is considered.

Figure 1 shows the Buck converter fed by a (possibly non-constant) dc-voltage power supply (on the left) and connected to a load (on the right). With abuse of notation all the variables and functions given in this topological representation will be used in the state-equation model even though their time evolutions in both representations would differ, as the circuit topology contains an idealized switch and the state-equations assume a smooth variation of the supply voltage on the terminals of the converter.

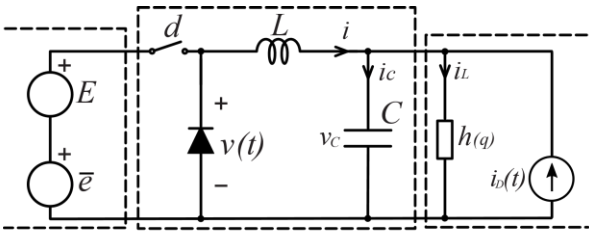

Figure 1: Buck converter with disturbances

The load side is modelled as the parallel connection of a generic dissipative nonlinear load and a current source. The volt-ampère law $i_L = g(v_C) = g\left(\frac{q}{C}\right) = h(q)$ (with q the capacitor charge) of the static dipole is assumed known, and the technical assumption of $h(q)$ a monotone non-decreasing nonlinear function is made. The current source models an unknown independent disturbance $i_D(t) = \overline{i_D} + \widetilde{i_D}(t)$. Here, as well as everywhere else in the paper, a bar and a tilde over a variable indicate, respectively, a constant component and a bounded variation of its value.

Taking the flux linkage in the inductance and the capacitor charge as state variables, the following average state-equation model can be derived, where v(t) is the average voltage across the diode, calculated as $\mathrm{v(t)} = \mathrm{d(t)} \cdot [\mathrm{E} + \bar{\mathrm{e}}]$, with d(t) the duty-cycle of the binary signal commanding the ideal switch.

$$\begin{aligned} \dot{\psi} &= -\frac{q}{C} + v(t) \\ \dot{q} &= \frac{\psi}{L} - h(q) + i_D(t) \end{aligned} \qquad (1)$$

Remark 1: In the sequel the first step in designing the controller will be considering the signal $\mathrm{v(t)} = \mathrm{d(t)}\big(\mathrm{E} + \mathrm{e(t)}\big)$ as its output. The true control variable, i.e., the duty-cycle signal $d(t)$ will be designed in a second step. Notice that this latter signal is constrained to the interval $(0, 1)$. As only the CCM is considered and $d(t) \in (0,1)$, the following holds:

$$\begin{aligned} & i_L = \frac{\psi}{L} > 0 \\ & E > v_C = \frac{q}{C} \geq 0 \end{aligned} \qquad (2)$$

2.2. Specifications of closed-loop behaviour

The following problem of output regulation with disturbance rejection has to be solved:

1. Global asymptotic stabilization of the desired equilibrium point (EP) under the solely presence of the constant disturbances $\bar{e}, \overline{i_D}$, where the EP is characterized as follows:

$\overline{v_C} = v_e$, specified constant $\Rightarrow \bar{q} = q_e = C \cdot v_e$
$\bar{\psi} = L \cdot \bar{\imath} = L \cdot [h(q_e) - \overline{i_D}]$

2. Ultimately bounded stability of $(\bar{\psi}, \bar{q})$ under the additional presence of the bounded variable disturbance signal $\widetilde{i_D}(t)$, i.e. ISS with respect to this disturbance.

3. CONTROLLER DESIGN

3.1. Desired closed loop dynamics

The problem is formulated in the state-space proposing a first order dynamic extension (state x_3 in the closed loop model) and a feedback control law $v(\psi, q, x_3)$ such that the desired equilibrium point is Globally Asymptotically Stable (GAS) (up to the restrictions (2)). *Disregarding the varying* part of the load-side disturbance, i. e., considering only the constant part of it, this desired closed-loop dynamics (CLD) is a-priori proposed as the following PHS:

$$\begin{bmatrix} \dot{x_1} \\ \dot{x_2} \\ \dot{x_3} \end{bmatrix} = \underbrace{\begin{bmatrix} S_{11} & S_{12} & S_{13} \\ -S_{12} & S_{22}(q) & S_{23} \\ -S_{13} & -S_{23} & S_{33} \end{bmatrix}}_{S(x_2)} \cdot \begin{bmatrix} \frac{\partial H(x)}{\partial x_1} \\ \frac{\partial H(x)}{\partial x_2} \\ \frac{\partial H(x)}{\partial x_3} \end{bmatrix} \qquad (3)$$

with $S_{ii} < 0,\ i = \{1,2,3\}$; $\forall\, x_2$

$$H(x_1, x_2, x_3) = \frac{1}{2} \cdot \left(\frac{x_1^2}{L_1} + \frac{x_2^2}{C_2} + \frac{(x_3 - \alpha)^2}{K_I}\right) \qquad (4)$$

with the constants $L_1, C_2, K_I > 0$

And the satisfaction of the following conditions:

$$\alpha = -\frac{K_I S_{13} i_D}{S_{13} S_{23} - S_{33} S_{12}} \qquad (5)$$

$$S_{23} = -\frac{S_{12}}{S_{13}}\left[\frac{C_2}{L_1 g_2}(S_{13}^2 + S_{11} S_{33}) - S_{33}\right] \qquad (6)$$

$$S_{22}(q) = -g_2 - C_2 \frac{h(q) - h(q_e)}{q - q_e}\,; \qquad (7)$$

with the constant $g_2 > 0$

ISBN 978-88-97999-88-1; Bruzzone, Dauphin-Tanguy, and Junco Eds.

It can be seen that a positive definite storage function $H(x_1, x_2, x_3)$ has been chosen, with its minimum located at $(x_1, x_2, x_3) = (0,0,\alpha)$.

Remark 2: Equations (3), (4) and (5) define a PHS whose equilibrium point $(x_1, x_2, x_3) = (0,0,\alpha)$ is asymptotically stable. Indeed, referring to the standard notation $\dot{x} = (\boldsymbol{J} - \boldsymbol{R})\frac{\partial H(x)}{\partial x}$, the decomposition $\boldsymbol{S}(q) = \boldsymbol{J} - \boldsymbol{R}$ explicitly shows the antisymmetric interconnection matrix $\boldsymbol{J}$ and the positive definite matrix $\boldsymbol{R}$, defined as follows:

$$\boldsymbol{J} = \begin{bmatrix} 0 & S_{12} & S_{13} \\ -S_{12} & 0 & S_{23} \\ -S_{13} & -S_{23} & 0 \end{bmatrix}; \text{and } \boldsymbol{R} = \mathrm{diag}\{-S_{ii}\}$$

By virtue of the properties of $\boldsymbol{J}$ and $\boldsymbol{R}$, the orbital derivative of $H(x_1, x_2, x_3)$ is a negative definite function of $(x_1, x_2, x_3 - \alpha)$, meaning that the closed loop trajectories converge to $(0,0,\alpha)$ as time goes to infinite. This is shown by the following calculation demonstrating that $H(x_1, x_2, x_3)$ is a Lyapunov function for the equilibrium point:

$$\frac{dH(x)}{dt} = -\left(\frac{\partial H(x)}{\partial x}\right)^T \boldsymbol{R}\,\frac{\partial H(x)}{\partial x} < 0$$

3.2. Controller Design

3.2.1. Definition of the closed loop states

To obtain the control law, firstly we need to define the closed loop states, starting with the output regulation signal:

$$x_2 = q - q_e \tag{8}$$

Since q_e is considered constant, then:

$$\dot{x_2} = \dot{q} \tag{9}$$

Computing this identity taking $\dot{x_2}$ from (3) and $\dot{q}$ from (1), the following change of variables for x_1 is obtained:

$$x_1 = \frac{L_1}{S_{12}} \cdot \left[S_{22}(q)\frac{q-q_e}{C_2} + S_{23}\frac{x_3-\alpha}{K_I} - \bar{\iota_D} - \left(\frac{\psi}{L} - h(q)\right)\right] \tag{10}$$

Equations (8) and (10) are now used to replace x_1 and x_2 in the dynamics of x_3 given in (3), that is:

$$\dot{x_3} = \frac{-S_{13}}{S_{12}} \cdot \left[S_{22}(q)\frac{q-q_e}{C_2} + S_{23}\frac{x_3-\alpha}{K_I} - \bar{\iota_D} - \left(\frac{\psi}{L} - h(q)\right)\right] - S_{23}\frac{q-q_e}{C_2} + S_{33}\frac{x_3-\alpha}{K_I} \tag{11}$$

Substituting the value of α from (5) in (11) and using (7), the state equation of x_3 may be written as:

$$\dot{x_3} = \frac{-S_{13}}{S_{12}} \cdot \left[-g_2\frac{q-q_e}{C_2} - \left(h(q) - h(q_e)\right) + S_{23}\frac{x_3}{K_I} - \left(\frac{\psi}{L} - h(q)\right)\right] - S_{23}\frac{q-q_e}{C_2} + S_{33}\frac{x_3}{K_I} \tag{12}$$

In this way, x_3 can be computed without using the information of the unknown constant disturbance $\bar{\iota_D}$.

Remark 3: The convergence $x_2 \to 0$ amounts to satisfying the regulation requirement for the output (capacitor) voltage $v_c \to \frac{q_e}{C} = v_e$, see Eq. (8).

Remark 4: The dynamic extension has been introduced in order to provide the integral action necessary to asymptotically reject load-side constant disturbances. It is well known that controller integrator outputs tend to constant values which depend on the value of the constant disturbance. In this case this is the convergence $x_3 \to \alpha$, where α depends on the disturbance magnitude, see Eq.(5). Notice that although the change of coordinates and the closed-loop PHS are written using the unknown disturbance, it is only in order to analyze the stability of the control system. Indeed, as it will be seen later, the controller finally implemented *does not* require the information of the disturbance.

Proposition 1: The asymptotic stability of the EP $(\overline{x_1}, \overline{x_2}, \overline{x_3}) = (0,0,\alpha)$ of system (3) implies the asymptotic stability of the EP $(\bar{\psi}, \bar{q})$ of the original system (1) under the action of a constant disturbance $i_D(t) = \bar{\iota_D}$.

Proof: The convergence of the output to its desired equilibrium value has been already established in Remark 3. It remains to show the convergence of the inductance flux to its equilibrium value $\bar{\psi}$. Recalling the equilibrium values of the x variables $(\overline{x_1}, \overline{x_2}, \overline{x_3}) = (0,0,\alpha)$ and using Eq. (10):

$$\overline{x_1} = 0 \Leftrightarrow \frac{L_1}{S_{12}} \cdot \left[S_{22}(x_2)\frac{\bar{q}-q_e}{C_2} + S_{23}\frac{\overline{x_3}-\alpha}{K_I} - \bar{\iota_D} - \left(\frac{\bar{\psi}}{L} - h(\bar{q})\right)\right] = 0 \Leftrightarrow \bar{\psi} = L(h(\bar{q}) - \bar{\iota_D}) \tag{13}$$

3.2.2. Computing the control law

The control law is calculated matching the expressions for $\dot{x_1}$ given in (3) and the one obtained via time differentiation of (10). The following auxiliary calculations lead to the desired matching equation (ME). First, from (3) we obtain the left side of it as:

$$\dot{x_1} = S_{11}\frac{x_1}{L_1} + S_{12}\frac{x_2}{C_2} + S_{13}\frac{x_3-\alpha}{K_I}$$

$$= \frac{S_{11}}{S_{12}}\left[S_{22}(q)\frac{q-q_e}{C_2} + S_{23}\frac{x_3-\alpha}{K_I} - \bar{\iota_D} - \left(\frac{\psi}{L} - h(q)\right)\right] + S_{12}\frac{q-q_e}{C_2} + S_{23}\frac{x_3-\alpha}{K_I}$$

Then, differentiating (10), and using (1) to replace $\dot{q}$ and $\dot{\psi}$ we obtain the right side for the ME:

$$\dot{x}_1 = \frac{L_1}{S_{12}}\left(\left[\frac{\partial S_{22}(q)}{\partial q} \cdot \frac{q-q_e}{C_2} + \frac{S_{22}(q)}{C_2}\right] \dot{q} + S_{23}\frac{\dot{x}_3}{K_I} - \frac{\dot{\psi}}{L} + \frac{\partial h(q)}{\partial q}\dot{q}\right)$$

$$= \frac{L_1}{S_{12}}\left(\left[\frac{\partial S_{22}(q)}{\partial q} \cdot \frac{q-q_e}{C_2} + \frac{S_{22}(q)}{C_2} + \frac{\partial h(q)}{\partial q}\right] \left(\frac{\psi}{L} - h(q) + \bar{\imath}_D\right) + S_{23}\frac{\dot{x}_3}{K_I} - \frac{1}{L}\left(v(t) - \frac{q}{C}\right)\right)$$

Now, the control input $v(t)$ is explicitly shown. If (7) holds, then:

$$\frac{\partial S_{22}(q)}{\partial q} \cdot \frac{q-q_e}{C_2} + \frac{S_{22}(q)}{C_2} + \frac{\partial h(q)}{\partial q} = -\frac{g_2}{C_2}$$

Now the ME can be written as follows:

$$\frac{S_{11}}{S_{12}}\left[S_{22}(q)\frac{q-q_e}{C_2} + S_{23}\frac{x_3-\alpha}{K_I} - \bar{\imath}_D - \left(\frac{\psi}{L} - h(q)\right)\right] + S_{12}\frac{q-q_e}{C_2} + S_{23}\frac{x_3-\alpha}{K_I} = \frac{L_1}{S_{12}}\left(\frac{-g_2}{C_2}\left(\frac{\psi}{L} - h(q) + \bar{\imath}_D\right) + S_{23}\frac{\dot{x}_3}{K_I} - \frac{1}{L}\left(v(t) - \frac{q}{C}\right)\right) \tag{14}$$

Recall x_3 is independent of α and $\bar{\imath}_D$. So, if (5) and (6) hold, the ME (14) together with Eq. (12) leads us to the following control law:

$$v(\psi, q, x_3) = \left[\left(\frac{\psi}{L} - h(q)\right)\left(\frac{L_1 S_{23} S_{13}}{S_{12}^2 K_I} - \frac{L_1 g_2}{S_{12} C_2} + \frac{S_{11}}{S_{12}}\right) + \frac{x_3}{K_I}\left(\frac{L_1 S_{23}}{S_{12} K_I}\left(S_{33} - \frac{S_{13}}{S_{12}}S_{23}\right) - \left(S_{13} + \frac{S_{11}}{S12}S_{23}\right)\right) + \left(\frac{q-q_e}{C_2}g_2 + h(q) - h(q_e)\right) \cdot \left(\frac{L_1 S_{23} S_{13}}{S_{12}^2 K_I} + \frac{S_{11}}{S_{12}}\right) - \frac{q-q_e}{C_2}\left(S_{12} + \frac{L_1 S_{23}^2}{K_I S_{12}}\right) + \frac{L_1}{L S_{12}}\frac{q}{C}\right]\frac{L S_{12}}{L_1} \tag{15}$$

Equation (15), together with the dynamics of x_3 given by (12), provides the feedback control law that produces the desired CLD of the open loop system (1).

The fulfillment of (5), (6) and (7) together with $S_{11}, S_{33} < 0$ ensures that the control law and the controller state dynamics are independent of $\bar{\imath}_D$ and α, and $S_{22}(q) < 0$, $\forall\, q$.

Remark 5: Notice that, despite its seeming complexity, the control law (15) is a simple linear expression up-to the need to reconstruct the load current in the controller through the nonlinear function $h(q)$. The same holds for the dynamics of x_3. In the implementation of the control law, instead of ψ and q, the inductor current i and the capacitor voltage v_c are to be used.

Remark 6: Recalling that the real control input is not $v(\psi, q, x_3)$ but the duty cycle signal $d(t)$ calculated as follows:

$$d(t) = \frac{1}{E} \cdot\ v(\psi, q, x_3) \tag{16}$$

it is recognized that for this controller to assure asymptotic stability the condition $\bar{e} = 0$ must be satisfied, i.e., the supply-side disturbance must be zero. This shortcoming will be removed supplementing this controller with a PI-regulator acting on the output error (see subsection 3.4).

3.3. Rejection of load-side time-varying disturbances

When considering the time varying disturbance $\tilde{\imath}_D(t)$ acting on the load side, i.e., the whole disturbance $i_D(t) = \bar{\imath}_D + \tilde{\imath}_D(t)$, the PHS (3) no longer the closed-loop dynamics, as it is driven by the disturbance as specified in (17):

$$\dot{x} = \boldsymbol{S}(x_2) \cdot \frac{\partial H(x)}{\partial x} + \begin{bmatrix} d_{x1} \\ d_{x2} \\ 0 \end{bmatrix} \tag{17}$$

where the driving inputs $d_{x1,2}$ depend on the disturbance $\tilde{\imath}_D(t)$ acting on the open loop system (1) as follows:

$$\begin{bmatrix} d_{x1} \\ d_{x2} \\ 0 \end{bmatrix} = \begin{bmatrix} -\frac{L_1 g_2}{S_{12} C_2} \cdot \tilde{\imath}_D(t) \\ \tilde{\imath}_D(t) \\ 0 \end{bmatrix} \tag{18}$$

Proposition 2: System (1) in closed loop with the controller given by Eq. (15) and Eq. (12) is Input-to-State-Stable (ISS) (Khalil, 2002) with respect to the bounded disturbance $\tilde{\imath}_D(t)$.

Proof: First we compute the time derivative of $H(x)$, considering the disturbances $d_{x1,2}$, i.e., the dynamics (17):

$$\dot{H}(x) = \frac{S_{11} x_1^2}{L_1^2} + \frac{S_{22}(x_2) x_2^2}{C_2^2} + \frac{S_{33}(x_3-\alpha)^2}{K_I^2} + \frac{x_1}{L_1}d_{x1} + \frac{x_2}{C_2}d_{x2} \tag{19}$$

Recalling that $S_{11} < 0$, $S_{33} < 0$ and $S_{22}(x_2) \le -g_2$, replacing $d_{x1,2}$, and using the following auxiliary fact (written for some generic variables γ, ω)

$$-a\gamma^2 + b\gamma\omega \le -\frac{a}{2}\gamma^2 + \frac{2\,b^2}{a}\omega^2\ ; \quad \text{with } a, b > 0$$

the following inequalities can be obtained:

$$\frac{S_{11} x_1^2}{L_1^2} + \frac{x_1}{L_1}d_{x1} \le \frac{-|S_{11}|}{2L_1^2}x_1^2 + \frac{2}{|S_{11}|}\left(\frac{-L_1 g_2}{S_{12} C_2}\right)^2 \tilde{\imath}_D(t)^2$$
$$\frac{S_{22}(x_2) x_2^2}{C_2^2} + \frac{x_2}{C_2}d_{x2} \le -\frac{g_2}{2C_2^2}x_2^2 + \frac{2}{g_2}\tilde{\imath}_D(t)^2$$

Thus, the following inequality for $\dot{H}(x)$ can be written:

$$\dot{H}(x) \le \frac{-|S_{11}|}{2L_1^2}x_1^2 + \frac{2}{|S_{11}|}\left(\frac{-L_1 g_2}{S_{12}C_2}\right)^2 \tilde{i_D}(t)^2 - \frac{g_2}{2C_2^2}x_2^2 + \frac{2}{g_2}\tilde{i_D}(t)^2 + S_{33}\frac{(x_3-\alpha)^2}{K_I^2} \quad (20)$$

Defining:

$$\lambda_1 = \text{mín}\left\{\frac{|S_{11}|}{2L_1^2}\,;\frac{g_2}{2C_2^2}\,;\,\frac{|S_{33}|}{K_I^2}\right\},\ \lambda_1 > 0$$

$$\lambda_2 = \frac{2}{|S_{11}|}\left(\frac{L_1 g_2}{S_{12}C_2}\right)^2 + \frac{2}{g_2}\ ,\ \lambda_2 > 0 \quad (21)$$

$$\chi = \begin{bmatrix} x_1 \\ x_2 \\ x_3 - \alpha \end{bmatrix}$$

$$\dot{H}(\chi) \le -\lambda_1|\chi|^2 + \lambda_2\,\tilde{i_D}(t)^2 \quad (22)$$

Eq. (22) completes the proof.

3.4. Rejection of supply-side disturbances

As seen in Figure 1, the supply voltage assumes a constant known value E (rated voltage of the source) plus an unknown (possibly piece-wise) constant disturbance value $\bar{e}$.

There are many applications where the mean value $\bar{e}$ is very small or directly zero, but there are others where it is of paramount importance, for instance, the case of solar PV arrays providing energy to a load through the converter system. This shows the importance of having a controller able to reject both disturbance inputs, $i_D(t) = \bar{i_D} + \tilde{i_D}(t)$ and also $\bar{e}$, thus assuring the ISS stability of the EP. This property can be achieved enhancing the control law with an additional PI action processing the output error. This yields the following expression for the duty-cycle (recall that $\frac{x_2}{C} = \frac{q-q_e}{C} = v_c - \bar{v}$):

$$d(t) = \frac{1}{E}\cdot\left(v(\psi, q, x_3) + K_{pi}\frac{x_2}{C} + K_{ii}\int\frac{x_2}{C}dt\right) \quad (23)$$

where E is the constant voltage of the source, which is not measured, but programmed as its rated value for the calculation of $d(t)$.

Remark 7: To maintain the properties of the control law (15) without the addition of the PI, the duty cycle had to be calculated not as shown in (16) but as $d(t) = \frac{1}{E+\bar{e}}\cdot v(\psi, q, x_3)$. This is not convenient (or possible, under certain circumstances) because it would imply equipping the system with one more sensor to measure the supply voltage.

4. VALIDATION THROUGH SIMULATION

The performance of the controller (15), (12) is tested via simulation. First, the controller is tested under design conditions and next in presence of constant and bounded time-varying disturbances and parameter dispersion in some key electrical components (load model and the value of the voltage source). The model of the load, which is graphically given in Figure 2, is:

$$h(q) = \left(\frac{v_C}{20}\right)^5 - \left(\frac{v_C}{20}\right)^3 + \left(\frac{v_C}{87}\right) + \text{atan}\left(\frac{v_C}{1.5}\right) \quad (24)$$

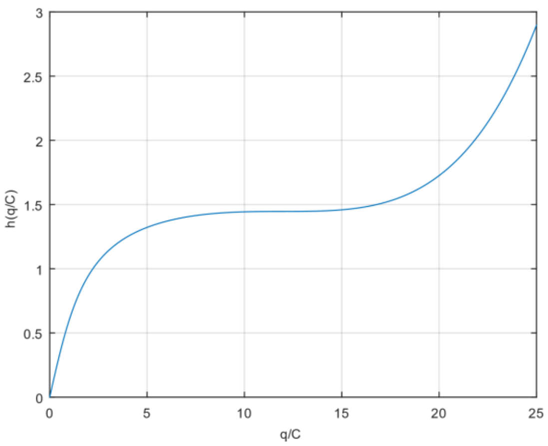

Figure 2: Nonlinear dissipative volt-ampère law

Thus, $h(q)$ is a nonlinear dissipative load (NLD) fulfilling the non-decreasing assumption. The parameters used in simulation of the Buck converter are taken from (Kwasinski and Krein 2007): $L = 500\,uH$, $C = 1000\,uF$ and $E = 22{,}2\,V$. The set of parameters for the controller are $S_{11} = -0{,}5$, $S_{12} = -1$, $S_{13} = -1$, $S_{23} = -1{,}195$, $g_2 = 3$, $S_{33} = -0{,}7$, $L_1 = 2L$, $C_2 = 1{,}1C$ and $K_I = 0{,}04$.

4.1. Controller analysis under design conditions

In this subsection the controller is tested under the design conditions. First, considering perfect knowledge of the model (1); next, introducing a constant disturbance $\bar{i_D}$; and, at last, a time-varying disturbance $\tilde{i_D}(t)$ to show the ISS property.

Experiment 1: The system starts with zero initial conditions. The capacitor voltage reference is set to $\bar{v} = 12V$. At $t = 70ms$ the voltage reference changes to $\bar{v} = 17V$. At time $t = 140ms$ a $50mA$ constant current load is connected in parallel with the NLD. The time response is shown in Figure 3.

Experiment 2: Same simulation scenario as Experiment 1. At $t = 25ms$ a bounded disturbance is injected: $\tilde{i_D}(t) = 0.5\frac{\bar{\psi}}{L}sin(2\pi 50t)$ is injected. In presence of $\tilde{i_D}(t)$, the capacitor voltage reference is changed and the constant current load is connected. The time response is shown on Figure 4.

The controller asymptotically stabilizes the desired equilibrium point, even under the presence of a *constant* load-side disturbance. This feature is provided by the dynamic extension, conceived to reject that type of disturbances. The ISS property, i.e., the bounded response under the action of a bounded disturbance, can be observed in the last set of simulations.

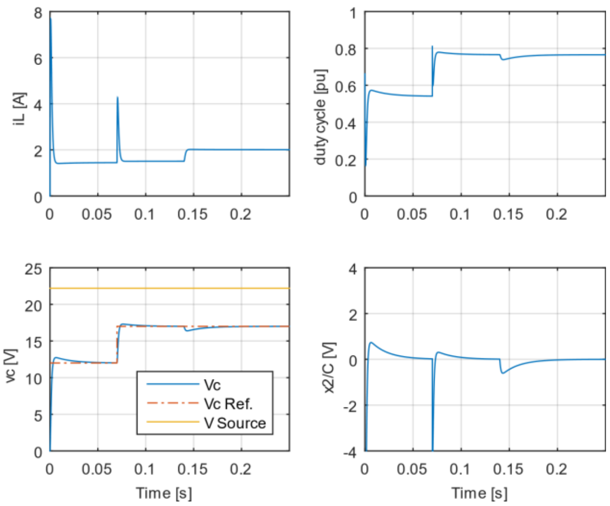

Figure 3: Time responses of Experiment 1.

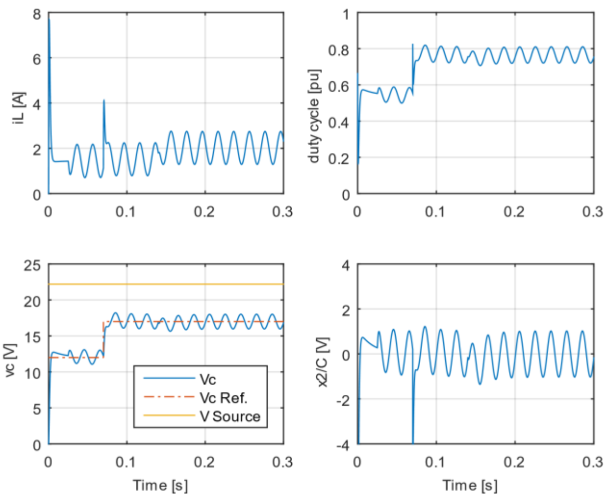

Figure 4: Time responses of Experiment 2.

4.2. Disturbances on supply-side

First, the non-robustness of the control law configured by {(15), (12),(16)} respect to supply-side disturbances is shown. Later, the rejection by the outer PI-loop of piece-wise constant disturbances acting on this side is demonstrated.

4.2.1. Performance degradation of controller {(16), (12),(17)}

This controller, designed to reject load side disturbances, is tested now under the presence of a supply-side disturbance.

Experiment 3: For this experiment $i_D(t) = 0$. The voltage source value is $19{,}98\,V$, (90% of $22{,}2\,V$). Recall that the controller uses $E = 22{,}2\,V$ to calculate the duty cycle.

It is obvious from Figure 5 that the presence of a disturbance $e(t) = \bar{e}$ changes the EP of the closed loop to a different one, with $\overline{x_1} \neq 0$ and $\overline{x_2} \neq 0$. This is because the duty cycle is miscalculated under the effect of the unknown value $\bar{e}$.

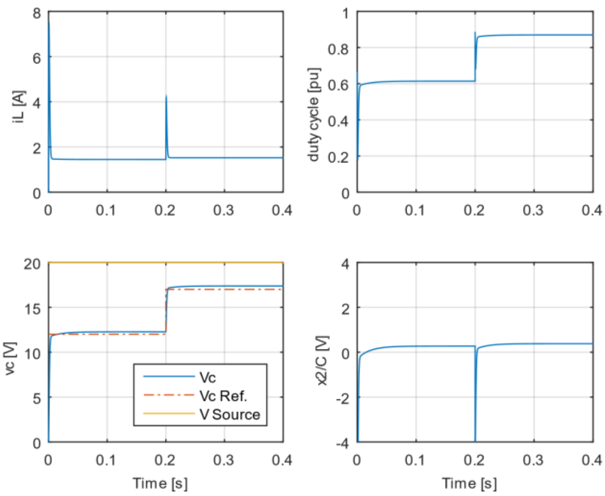

Figure 5: Time responses of Experiment 3

4.2.2. Supply-side disturbance rejection

An additional integral action is performed in order to reject $\bar{e}$, see Eq. (23).

Experiment 4: The simulation scenario is the same as Experiment 3*:* , but now the duty cycle is calculated using Eq. (23). The parameters of the additional PI controller are: $K_{pi} = 0{,}75$ and $K_{ii} = 1/0{,}03$.

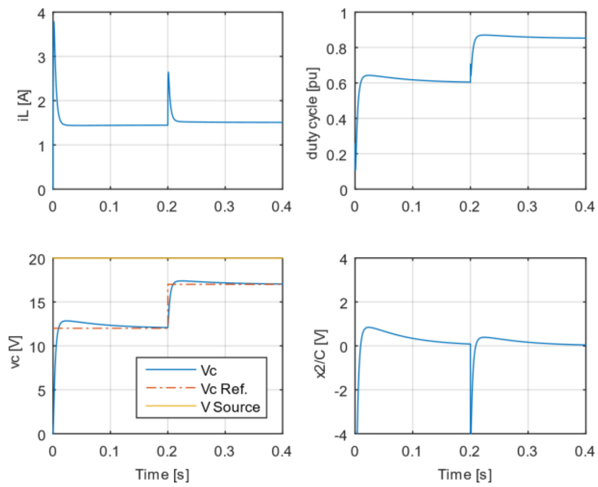

Figure 6: Times responses of Experiment 4.

Using Eq. (23), $\bar{e}$ is rejected, but the response of the whole system becomes slower. This is because the additional PI is tuned to be slower than the closed loop system (3).

4.3. Disturbances on load- and supply-sides

The objective of the experiment below is to show that the controller (15), (12) enhanced with an additional PI controller (Eq. (23)) can reject constant disturbances on both sides and preserves the ISS property with respect to load side time varying bounded disturbances.

We also introduce now a state dependent disturbance: changing the model of the load connected to the output of the Buck converter by the following one, see also Figure 7:

$$h(q) = \left(\frac{v_C}{20}\right)^5 - \left(\frac{v_C}{17}\right)^3 + \left(\frac{v_C}{87}\right) + \text{atan}\left(\frac{v_C}{1.5}\right) \quad (25)$$

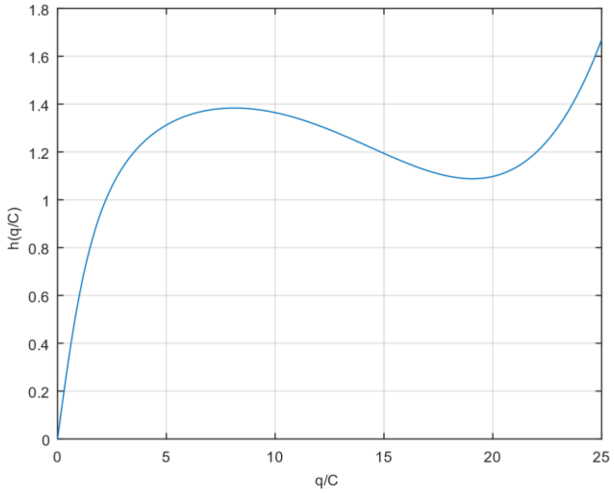

Figure 7: Volt-ampère law of nonlinear load for Experiment 5.

The controller remains programmed with the load model given by Eq. (24). Notice that this load does not fulfill the non-decreasing assumption, which can be relaxed as long as $S_{22}(q) < 0, \forall\, q$. This implies that g_2 must be bigger enough to ensure it.

Experiment 5: The voltage reference, initially set to $12\,V$, changes to $16\,V$ at $t = 0{,}15s$ (notice that both reference values are in the decreasing volt-ampère zone of the load model). The supply-side disturbance is the same as in the previous experiment. At time $t = 0{,}3s$ a $50\,mA$ constant current load is connected in parallel with the load, and at time $t = 0{,}5s$ a bounded load side disturbance $\tilde{\iota_D}(t)$ is injected (same as Experiment 2).

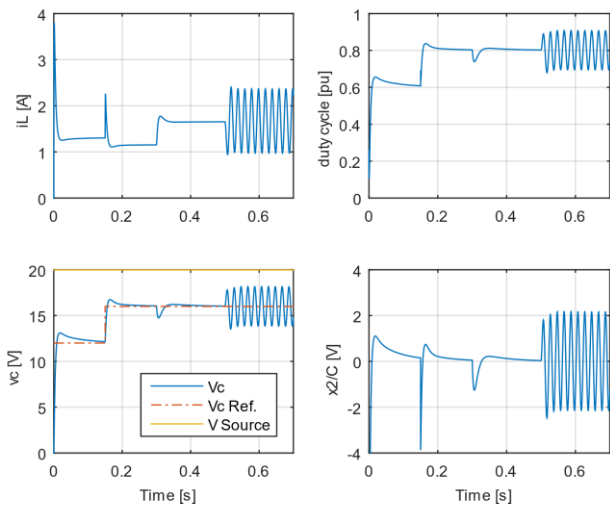

Figure 8: Time responses of Experiment 5.

The desired equilibrium point is stabilized, under the presence of disturbances acting on both sides, and the ISS property is conserved.

5. CONCLUSIONS

A dynamic controller assuring global asymptotic stability of the desired equilibrium point of a DC-DC Buck converter has been designed. On the basis of a nonlinear averaged state-equation model, the control system design was achieved proposing a closed-loop PHS target model having a positive definite energy function and dissipation in all its states, making it a Lyapunov function for any desired equilibrium point. It has been shown that this design guarantees ISS stability regarding (possible varying) bounded disturbances on the load-side. An outer PI-loop was added in order to reject also piece-wise constant disturbances on the supply-side. Simulation experiments confirm the correct performance of the overall controller.

Further work includes increasing by one the order of the dynamic extension embodied in the closed-loop PHS in order to be able to reject supply-side disturbances without adding a classical PI outer loop. Also of interest is extending the results to other kind, possibly dynamic and/or non passive loads, as well as applying the methodology to other topologies of power electronic DC-DC converters. In view of the controller practical implementation, testing and tuning the closed-loop performance on a hybrid model where the control input is provided by a switch driven by a PWM-modulated continuous duty cycle is also planned, as well as performing experimental validation tests.

ACKNOWLEDGMENTS

The authors wish to thanks SeCyT-UNR (the Secretary for Science and Technology of the National University of Rosario) and ANPCyT for their financial support through projects PID-UNR 1ING502 and FONCyT PICT 2012 Nr. 2471, respectively.

REFERENCES

Bacha S., Munteanu I., Bratcu A., 2014. Power Electronic Converters Modelling and Control: with Case Studies. London: Springer

Dong Tan F., 2013. Address from the Editor-in-Chief of the IEEE J. Emerging & Selected Topics in Power Electronics. Available from: http://www.ieee-pels.org/publications/jstpe [accessed 15 May 2016].

Khalil, H., 2002. Nonlinear Systems Second Edition. New Jersey: Prentice-Hall.

Kwasinski, A., Krein, P. T., 2007. Passivity-based control of Buck converters with constant-power loads. Power Electronics Specialists Conference, PESC 2007. IEEE, pp. 259-265, 17-21 June 2007, Orlando, FL.

Ortega R., van der Schaft A., Maschke B., Escobar G., 2002. Interconnection and damping assignment passivity-based control of port-controlled Hamiltonian systems. Automatica, Volume 38, Issue 4: pp. 585–596.

Sira-Ramírez H., Silva-Ortigoza R., 2006. Control Design Techniques in Power Electronics Devices. London: Springer-Verlag

Tan S. C., Lai Y. M, Tse, C. K., Cheung, M. K. H., 2006. Adaptive feedforward and feedback control schemes for sliding mode controlled power converters. IEEE Trans. Power Electron., vol. 21: no. 1, pp. 182–192.

AUTHORS BIOGRAPHY

Sergio Junco received the Electrical Engineer degree from the *Universidad Nacional de Rosario* (UNR) in 1976. In 1982, after 3 years in the steel industry and a 2-year academic stage at the University of Hannover, Germany, he joined the academic staff of UNR, where he currently is a Full-time Professor of System Dynamics and Control and Head of the Automation and Control Systems Laboratory. His current research interests are in Modelling, simulation, control and diagnosis of dynamic systems, with applications in the fields of motion control systems with electrical drives, power electronics, mechatronics, vehicle dynamics and smart grids. He has developed, and currently teaches, several courses at both undergraduate and graduate level on System Dynamics, Bond Graph Modelling and Simulation, Advanced Nonlinear Dynamics and Control of Electrical Drives, as well as Linear and Nonlinear Control with Geometric Tools.

Juan Tomassini was born in Rosario, Argentina. He received his degree in Electrical Engineering from the Universidad Nacional de Rosario (UNR), Argentina, in 2013. He worked as an electrical generation programmer in the administrator company of the wholesale electricity market (CAMMESA). Since September 2014 he has been a PhD student in Electrical Engineering and Control at the Faculty of Engineering (FCEIA) of UNR. His work is supported by the Nacional Agency for Scientific and Technological Promotion (ANPCyT). His main research interests are on IDA-PBC control, renewable energy and smart grids.

Alejandro G. Donaire was born in Rosario, Argentina. He received the Electronic Engineering and PhD degrees in 2003 and 2009, respectively, both from the Universidad Nacional de Rosario (UNR), Argentina. His work was supported by the Argentine National Council of Scientific and Technical Research, CONICET. In 2009, he joined the Centre for Complex Dynamic Systems and Control, The University of Newcastle, Australia. From 2015 to March 2017 he was with the PRISMA Lab at the Università degli Studi di Napoli Federico II. He recently joined the Institute for Future Environments, School of Electrical Engineering and Computer Science, Queensland University of Technology, Australia. His research interests include nonlinear and energy-based control theory with application to electrical drives, multi-agent systems, robotics, smart micro-grids networks, marine and aerospace mechatronics, and power systems.